Mechanistic Insight into the Protonolysis of the Pt−C Bond as a Model for C−H Bond Activation by Platinum(II) Complexes

Raffaello Romeo* and Giuseppina D'Amico

Dipartimento di Chimica Inorganica, Chimica Analitica e Chimica Fisica, and CIRCMSB, Università di Messina, Salita Sperone, 31, Vill. S. Agata, 98166 Messina, Italy

Received March 7, 2006

The kinetic and NMR features of the protonolysis reactions on platinum(II) alkyl complexes of the types *cis*-[$PtMe_2L_2$], [$PtMe_2$(L-L)], *cis*-[PtMeClL$_2$], and [PtMeCl(L-L)] (L = PEt_3, $P(Pr^i)_3$, PCy_3, $P(4\text{-MePh})_3$, L-L = dppm, dppe, dppp, dppb) in methanol suggest a rate-determining proton attack at the Pt−C bond. In contrast, a multistep oxidative-addition−reductive-elimination mechanism characterizes the methane loss on protonation of the corresponding *trans*-[PtMeClL$_2$] species. Tools that were particularly diagnostic in suggesting different reaction pathways for the two systems were (i) the different results of kinetic deuterium isotope experiments, (ii) the detection or absence of Pt(IV) hydrido alkyl intermediate species by low-temperature ^{1}H NMR experiments, and (iii) the detection or absence of isotope scrambling and incorporation of deuterium into Pt−CH_3, combined with the loss of a range of CH_nD_{n-4} isotopomers. For all systems, the rates of protonolysis are retarded by ligand steric congestion, accelerated by ligand electron donation, and almost unaffected by the chain length along the series of chelate complexes. A straight line correlates the rates of protonolysis of *cis*-dialkyl and *cis*-monoalkyl complexes, the difference in reactivity between the two systems being almost 5 orders of magnitude (slope of the line = 6×10^4). Factors controlling the dichotomy of behavior between complexes of different geometry have been taken into consideration. Application of the principle of microscopic reversibility suggests the reason why platinum complexes with nitrogen donor ligands appear to be far more efficient than platinum phosphane complexes in activating the C−H bond.

Introduction

The mechanism of electrophilic cleavage of metal−carbon bonds in transition-metal complexes is especially intriguing, because of the problem of the selectivity of the site attack. This complicating feature is shown particularly well in Pt(II) protonolysis chemistry. Protonation may take place by (i) a concerted attack at the metal−carbon bond (S_E2 mechanism), as for electrophilic substitution on main-group organometallics,[1] or (ii) a stepwise prior oxidative addition on the central metal followed by reductive elimination (S_E(ox) mechanism),[2] as illustrated approximately in Scheme 1. Other reaction pathways, typical of alkyl mercury compounds[3] or of metals that do not have an accessible higher oxidation state, can in principle take place. These include concurrent attack of the two ends of the reagent on the polarized metal−carbon bond, forming cyclic or open transition states, or attack at the aromatic ring in the case of metal−aryl derivatives.[4] For instance, the S_E(ox) mechanism is unlikely for Au(III) because of the unavailable +5 oxidation state,[5] and an S_E2 mechanism is consistent with the experimental findings. The reverse applies to Pt(II), where Pt(IV) is easily accessible.

Scheme 1. Alternative Reaction Pathways for Electrophilic Attack of the Proton at Alkylplatinum(II) Complexes

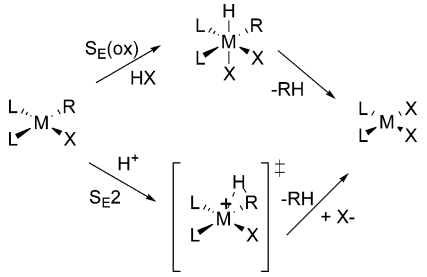

It is difficult to decide from kinetic evidence alone whether the attack of the proton commences at one or the other center, and it becomes impossible if the mechanism entails a rate-determining proton transfer. Early kinetic investigations on the protonolysis of platinum compounds focused almost exclusively on platinum(II) halo alkyl, diaryl, and alkyl aryl complexes containing the soft donor phosphanes, and the factors taken into consideration, among others, to support a given reaction pathway include (i) the form of the rate law, (ii) the halide ion dependence, (iii) the magnitude and sign of the entropies and volumes of activation, (iv) competition experiments, (v) the relative energies of the Pt−C σ-bonding MO and nonbonding 5d orbitals, (vi) the selectivity of alkyl vs aryl cleavage in mixed alkyl

* To whom correspondence should be addressed. Tel: +39-090-6765717. Fax: +39-090-393756. E-mail: rromeo@unime.it.

(1) (a) Abraham, M. H. In *Comprehensive Chemical Kinetics*; Bamford, C. H., Tipper, C. F. H., Eds.; Elsevier: Amsterdam, 1973. (b) Eaborn, C. *J. Organomet. Chem.* **1975**, *100*, 43. (c) Kochi, J. K. *Organometallic Mechanisms and Catalysis*; Academic Press: New York, 1978; pp 292−340.

(2) Johnson, M. D. *Acc. Chem. Res.* **1978**, *11*, 57.

(3) (a) Barone, V.; Bencini, A.; Totti, F.; Uytterhoeven, M. G. *Organometallics* **1996**, *15*, 1465. (b) Barbaro, P.; Cecconi, F.; Ghilardi, C. A.; Midollini, S.; Orlandini, A.; Vacca, A. *Inorg. Chem.* **1994**, *33*, 6163. (c) Nugent, W. A.; Kochi, J. K. *J. Am. Chem. Soc.* **1976**, *98*, 5979. (d) Jensen, F. R.; Rickborn, B. *Electrophilic Substitution of Organomercurials*; McGraw-Hill: New York, 1968.

(4) (a) Canty, A. J.; van Koten, G. *Acc. Chem. Res.* **1995**, *28*, 406. (b) Kalberer, E. W.; Houlis, J. F.; Roddick, D. M. *Organometallics* **2004**, *23*, 4112.

(5) Nyholm, R. S.; Vrieze, K. *J. Chem. Soc.* **1965**, 5337.

10.1021/om060217n CCC: $33.50
Publication on Web 06/09/2006

Chart 1. Sketch of the Halide-Assisted Transition State in an S_E2 Mechanism

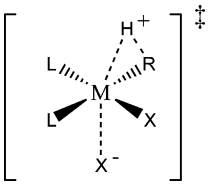

aryl complexes, and finally, (vii) the observed dependence of the rates upon the structural properties of these organometallic compounds.[6] A particular emphasis has been placed on the results of deuterium isotope experiments, as a diagnostic tool for the extent of proton involvement in the formation of the transition state.[6c,e,g] There is no general consensus on the operation of a common mechanism. According to the S_E(ox) mechanism, the halide-dependent term in the rate law was thought to reflect stabilization of the Pt(IV) intermediate by halide coordination. On the other hand, a fast preequilibrium between the uncharged substrate and X^-, combined with slow protonation and breakage of the metal−carbon σ bond, accounted for a variety of the observed cases, including linear, nonlinear, no dependence, and even retardation of the rate on [X^-] (Chart 1).

After the isolation of some platinum(IV) aryl hydrido complexes,[7] in 1995 three different groups reported that protonation of [$PtMe_2$(N-N)] complexes (N-N = 2,9-dimethyl-1,10-phenanthroline;[8] N-N = 2,2′-bipyridine, 4,4′-di-*tert*-butyl-2,2′-bipyridine, 1,10-phenanthroline[9]) or [$Pt(CH_2Ph)Cl$(N-N)] complexes (N-N = *N*,*N*,*N*′,*N*′-tetramethylethylenediamine[10]) with HX leads to the formation of platinum(IV) alkyl hydrido species that were isolated as solids[8] or detected as transient intermediates using low-temperature ^{1}H NMR spectroscopy[9,10] before their reductive elimination, at higher temperatures, to yield the corresponding monoorgano or dihalide compounds. Since then, the path to detection and characterization of stable platinum(IV) methyl hydrido complexes has been open, especially with the use of ligands that do not easily dissociate.[11] Formation of platinum(IV) alkyl hydrido species was not limited to diamine- or diimine-containing Pt(II) species. Addition of HCl to a CD_2Cl_2 solution of *trans*-[$PtMeCl(PEt_3)_2$] at −78 °C generates [$PtMe(H)Cl_2(PEt_3)_2$].[12] Addition of DOTf in CD_3OD at −78 °C revealed another phenomenon, incorporation of deuterium into the Pt−CH_3 site of unreacted *trans*-[$PtMeCl(PEt_3)_2$]. All these findings are against an S_E2 mechanism and strongly support a multistep S_E(ox) mechanism which was thought to involve (i) reversible chloride- or solvent-mediated protonation of Pt(II) to produce the observed Pt(IV) hydrido alkyl intermediate, (ii) reversible solvent or chloride dissociation, yielding a five-coordinate platinum(IV) species, and (iii) reductive C−H bond formation to give a σ-alkane complex which eventually loses alkane through either an associative or dissociative substitution pathway.[12] The nature of the solvent or of the ancillary ligands will influence the stability of the intermediates and transition states and, therefore, will dictate the choice of the rate-determining step.

Unmistakable evidence for the operation of an S_E(ox) mechanism for systems containing hard ligands (nitrogen donor atoms) or weak trans-activating groups (such as Cl^- in *trans*-[$PtMeCl(PEt_3)_2$]) does not necessarily imply that this multistep mechanism *accounts for protonolysis in all platinum(II) systems.* All of the previous experimental findings for electron-rich *cis*-dialkyl, *cis*- and *trans*-diaryl, and mixed aryl−alkyl phosphane complexes of platinum(II), and in particular the largely negative values for volumes and entropies of activation,[13] together with the largely positive isotope effect mentioned before, provide strong evidence that the primary kinetic step in the protonolysis pathway is a *one-step proton transfer* to the substrate.

In view of the fundamental mechanistic relevance of the protonation of the Pt−C bond as the *microscopic reverse* of C−H bond activation by platinum complexes,[12,14] we considered it of interest to perform a systematic examination of how changes in the Pt(II) ligand environment affect the protonolysis process. Thus, we studied in detail the kinetics of protonolysis of a series of dialkyl platinum(II) complexes of the types *cis*-[$PtMe_2L_2$] and [$PtMe_2$(L-L)] and monoalkyl complexes *cis*-[$PtMeClL_2$] and [PtMeCl(L-L)], and *trans*-[$PtMeClL_2$] (L = PEt_3, $P(Pr^i)_3$, PCy_3, P(4-MePh)$_3$; L-L = dppm, dppe, dppp, dppb) according to a protocol which includes the measurement of the dependence of the rate on proton and chloride concentration, the measurement of the primary deuterium isotope effect, the search for the presence of Pt(IV) intermediates or for deuterium incorporation into the methyl positions, and, in the case of the dialkyl complexes, the measurement of the rate dependence on the temperature. We can anticipate that *trans*-

(6) (a) Belluco, U.; Giustiniani, M.; Graziani, M. *J. Am. Chem. Soc.* **1967**, *89*, 6494. (b) Belluco, U.; Croatto, U.; Uguagliati, P.; Pietropaolo, R. *Inorg. Chem.* **1967**, *6*, 718. (c) Romeo, R.; Minniti, D.; Lanza, S.; Uguagliati, P.; Belluco, U. *Inorg. Chem.* **1978**, *17*, 2813. (d) Jawad, J. K.; Puddephatt, R. J. *Chem. Commun.* **1977**, 892. (e) Romeo, R.; Minniti, D.; Lanza, S. *J. Organomet. Chem.* **1979**, *165*, C36−C38. (f) Uguagliati, P.; Michelin, R. A.; Belluco, U.; Ros, R. *J. Organomet. Chem.* **1979**, *169*, 115. (g) Jawad, J. K.; Puddephatt, R. J.; Stalteri, M. A. *Inorg. Chem.* **1982**, *21*, 332. (h) Belluco, U.; Michelin, R. A.; Uguagliati, P.; Crociani, B. *J. Organomet. Chem.* **1983**, *250*, 565 (i) Alibrandi, G.; Minniti, D.; Romeo, R.; Uguagliati, P.; Calligaro, L.; Belluco, U.; Crociani, B. *Inorg. Chim. Acta* **1985**, *100*, 107. (j) Alibrandi, G.; Minniti, D.; Romeo, R.; Uguagliati, P.; Calligaro, L.; Belluco, U. *Inorg. Chim. Acta* **1986**, *112*, L15. (k) Alibrandi, G.; Minniti, D.; Monsù Scolaro, L.; Romeo, R. *Inorg. Chem.* **1988**, *27*, 318. (l) Yang, D. S.; Bancroft, G. M.; Bozek, J. D.; Puddephatt, R. J.; Tse, J. S. *Inorg. Chem.* **1989**, *28*, 1.

(7) (a) Wehman-Ooyevaar, I. C. M.; Grove, D. M.; van der Sluis, P.; Spek, A. L.; van Koten, G. *J. Chem. Soc., Chem. Commun*. **1990**, 1367. (b) Wehman-Ooyevaar, I. C. M.; Grove, D. M.; Kooijman, H.; van der Sluis, P.; Spek, A. L.; van Koten, G. *J. Am. Chem. Soc.* **1992**, *114*, 9916. (c) Wehman-Ooyevaar, I. C. M.; Grove, D. M.; de Vaal, P.; Dedieu, A.; van Koten, G. *Inorg. Chem.* **1992**, *31*, 5484.

(8) De Felice, V.; De Renzi, A.; Panunzi, A.; Tesauro, D. *J. Organomet. Chem.* **1995**, *488*, C13−C14.

(9) Hill, G. S.; Rendina, L. M.; Puddephatt, R. J. *Organometallics* **1995**, *14*, 4966.

(10) Stahl, S. S.; Labinger, J. A.; Bercaw, J. E. *J. Am. Chem. Soc*. **1995**, *117*, 9371.

(11) (a) Puddephatt, R. J. *Coord. Chem. Rev.* **2001**, *219*−*221*, 157. (b) O'Reilly, S. A.; White, P. S.; Templeton, J. L. *J. Am. Chem. Soc.* **1996**, *118*, 5684. (c) Hill, G. S.; Puddephatt, R. J. *J. Am. Chem. Soc.* **1996**, *118*, 8745. (d) Reinartz, S.; White, P. S.; Brookhart, M.; Templeton, J. L. *Organometallics* **2000**, *19*, 3854. (e) Canty, A. J.; Fritsche, S. D.; Jin, H.; Patel, J.; Skelton, B. W.; White, A. H. *Organometallics* **1997**, *16*, 2175. (f) Prokopchuk, E. M.; Jenkins, H. A.; Puddephatt, R. J. *Organometallics* **1999**, *18*, 2861. (g) Prokopchuk, E. M.; Puddephatt, R. J. *Organometallics* **2003**, *22*, 787.

(12) Stahl, S. S.; Labinger, J. A.; Bercaw, J. E. *J. Am. Chem. Soc*. **1996**, *118*, 5961.

(13) Romeo, R.; Plutino, M. R.; Elding, L. I. *Inorg. Chem.* **1997**, *36*, 5909.

(14) (a) Lersch, M.; Tilset, M. *Chem. Rev.* **2005**, *105*, 2471. (b) Labinger, J. A.; Bercaw, J. E. *Nature* **2002**, *417*, 507−514. (c) Zhong, H. A.; Labinger, J. A.; Bercaw, J. E. *J. Am. Chem. Soc.* **2002**, *124*, 1378−1399. (d) Johansson, L.; Tilset, M.; Labinger, J. A.; Bercaw, J. E. *J. Am. Chem. Soc.* **2000**, *122*, 10846−10855. (e) Procelewska, J.; Zahl, A.; van Eldik, R.; Zhong, H. A.; Labinger, J. A.; Bercaw, J. E. *Inorg. Chem*. **2002**, *41*, 2808−2810. (f) Johansson, L.; Ryan, O. B.; Tilset, M. *J. Am. Chem. Soc.* **1999**, *121*, 1974−1975. (g) Johansson, L.; Ryan, O. B.; Römming, C.; Tilset, M. *J. Am. Chem. Soc.* **2001**, *123*, 6579−6590. (h) Johansson, L.; Tilset, M. *J. Am. Chem. Soc.* **2001**, *123*, 739−740. (i) Holtcamp, M. W.; Henling, L. M.; Day, M. W.; Labinger, J. A.; Bercaw, J. E. *Inorg. Chim. Acta* **1998**, *270*, 467−478. (j) Periana, R. A.; Taube, D. J.; Gamble, S.; Taube, H.; Satoh, T.; Fujii, H. *Science* **1998**, *280*, 560−564. (k) Wick, D. D.; Goldberg, K. I. *J. Am. Chem. Soc.* **1997**, *119*, 10235−10236.

[$PtMeClL_2$] complexes exhibit totally different mechanistic features compared to dialkyl and monoalkyl complexes of cis geometry. We are inclined to think that this mechanistic difference is difficult to fit into a unified mechanism (S_E2 or $S_E(ox)$ mechanism). Rather, the different kinetic behaviors offer valuable information on the role of trans-activating groups and of the ensuing polarization of the platinum−carbon bond in governing the selectivity of the proton attack, the form of the reaction profiles, and the stability of intermediates and transition states. Mechanistic implications of the mechanism of C−H bond activation by platinum(II) complexes will be discussed.

Results

Synthesis and Characterization of Complexes. The reaction illustrated in eq 1 is fast and clean, and the desired products can be obtained in high yield and purity, as reported previously for an extended series of phosphanes of relatively high basicity and low cone angle.[15]

$$cis\text{-}[PtMe_2(Me_2SO)_2] + 2L \rightarrow cis\text{-}[PtMe_2L_2] + 2Me_2SO \quad (1)$$

Complications arise, as for [$PtMe_2$(cod)],[16,17] only for the reactions with the most sterically demanding or poorly σ-donating phosphanes, because of the easy re-entry of the leaving sulfoxide. In such a case, a valid alternative seems to be the use as precursors of [$Pt_2Me_4(\mu\text{-}SMe_2)_2$] or of [$PtMe_2$(nbd)].[18] In the ^{1}H NMR spectra of **1a**−**8a** the phosphorus-coupled methyl resonance appears as an apparent triplet ($^3J_{PH} \approx 7$ Hz) due to virtual coupling. The $^{31}P\{^1H\}$ NMR spectra show a single resonance. The cis stereochemistry for **1a**−**4a** was clearly indicated by the low values observed for $^1J_{PtP}$ (∼1850 Hz), which are diagnostic for a phosphane ligand trans to an alkyl or aryl group.[19] The ^{31}P chemical shifts for **5a**−**8a** follow the pattern characteristic of chelated bis(tertiary phosphane) alkanes of ring size 4−7.[20] The abnormally low value of the coupling constant $^1J_{PtP}$ (1422 Hz) for **5a** is correlated to the bite-angle strain for the four-membered dppm ring.

Careful stoichiometric protonolysis of *cis*-[$PtMe_2L_2$] in nonpolar solvents usually gave clean and isolable monoalkyl products. This was not the case for complexes with the sterically demanding phosphanes PPr^i_3 and PCy_3, because of the spontaneous easy conversion of cis monoalkyl products to the corresponding trans isomers.[21] The characterization of **2b** and **3b** has been performed "in situ", using low-temperature ^{1}H and $^{31}P\{^1H\}$ NMR, soon after the addition of acid to **2a** and **3a.** The reaction of *trans*-[$PtMeCl(Me_2SO)_2$] with stoichiometric amounts of dppe, dppp, and dppb gave the required chelated compounds (**6b**−**8b**). The same procedure applied to dppm mainly gave the dimeric species [$PtMeCl(\mu\text{-dppm})]_2$ in high yield, as reported previously for the corresponding reaction of dppm with [PtMeCl(cod)][22] in benzene. Careful protonolyis of [$PtMe_2$(dppm)], using methanolysis of acetyl chloride as the source of the proton, proved to be a convenient route to the preparation of the pure monomer **5b**.[23] In compounds **1b**−**8b** the methylplatinum resonance appears as four peaks of equal intensity due to coupling with two nonequivalent ^{31}P atoms, with ^{195}Pt satellites. The two nonequivalent phosphane ligands can be distinguished on the basis of the different magnitudes observed for the $^1J_{PtP}$ coupling constants of the two ^{31}P resonances (low value for P_A trans to carbon, high value for P_B trans to chloride).

The remaining *trans*-[$PtMeClL_2$] complexes (**1c**−**4c**) were prepared by two reaction routes: (i) spontaneous isomerization in methanol of the corresponding cis-monoalkyl species for L = PEt_3, $P(4\text{-}MeC_6H_4)_3$ and (ii) reaction of a slight excess of phosphane with *trans*-[$PtMeCl(Me_2SO)_2$] for L = PPr^i_3, PCy_3. Both procedures proved to be fast and easy, but method (ii) is to be preferred when using bulky phosphanes. The NMR characterizations of these complexes are in good agreement with their structures. Selected NMR data for all complexes in the text are reported in Tables 1 and 2. A complete list and assignment of NMR data are given in Table S1 in the Supporting Information. Figure S1 in the Supporting Information displays typical ^{1}H and ^{31}P NMR features that are useful to distinguish between compounds of classes **a**−**c**, respectively.

Protonolysis of Dialkyl Complexes. (a) NMR Measurements. The cleavage of the first Pt−C bond in complexes **1a**−**8a** takes place according to the reaction

$$cis\text{-}[PtMe_2L_2] \xrightarrow[[Cl^-]]{[H^+]} cis\text{-}[PtMeClL_2] + CH_4 \quad (2)$$

The reaction is too fast to be followed by NMR, where an immediate and sharp change in the spectrum is observed on addition of the acid. The final cis product can be isolated by evaporation of the solvent in a synthetic workup or can be recognized by NMR, at low temperature when dealing with compounds with sterically demanding phosphanes (**2b** and **3b**). In this particular case the cis configuration that results from Pt−C bond breaking is hardly retained at room temperature because of a subsequent geometrical isomerization. Attempts to detect by low-temperature NMR the presence of possible platinum(IV) alkyl hydrido intermediates of the type [$PtMe_2(H)Cl_2L_2$] were unsuccessful. The addition of acid to **1a**−**8a**, according to the procedure described in the Experimental Section, leads exclusively to the quantitative formation of *cis*-[$PtMeClL_2$] and methane. The same result was obtained when Me_3SiCl in wet CD_2Cl_2 was used to give 1 equiv of HCl. Treatment of **1a**−**8a** in CD_3OD/CD_2Cl_2 (8/1) with DOTf (1/10) and LiCl at −70 °C results in the immediate formation of CH_3D and of the complexes **1b**−**8b**. Similar results were obtained by Holtcamp, Labinger, and Bercaw in the protonolysis and deuteriolysis of [$PtMe_2$(depe)].[24]

(b) Spectrophotometric Studies. Typical spectral changes are associated with the protonolysis of **1a**−**8a**. The reaction takes place in a single step according to eq 2. The systematic kinetics of these reactions were studied at different proton and chloride concentrations and required the use of stopped-flow techniques. The reaction rate is independent of the concentration of Cl^-, within a wide range of concentrations. At the concentrations of acid used, the reactions went to completion and excellent fits were obtained from the regression analysis of the absorbance

(15) Romeo, R.; Alibrandi, G. *Inorg. Chem.* **1997**, *36*, 4822−4830.
(16) Haar, C. M.; Nolan, S. P.; Marshall, W. J.; Moloy, K. G.; Prock, A.; Giering, W. P. *Organometallics* **1999**, *18*, 474−479.
(17) Butikofer, J. L.; Hoerter, J. M.; Peters, R. G.; Roddick, D. M. *Organometallics* **2004**, *23*, 400−408.
(18) Appleton, T. G.; Hall, J. R.; Williams, M. A. *J. Organomet. Chem.* **1986**, *303*, 139.
(19) (a) Allen, F. H.; Pidcock, A. *J. Chem. Soc. A* **1968**, 2700. (b) Appleton, T. G.; Clark, H. C.; Manzer, L. E. *Coord. Chem. Rev.* **1973**, *10*, 335.
(20) Garrou, P. E. *Chem. Rev.* **1981**, *81*, 229.
(21) Romeo, R. *Comments Inorg. Chem.* **2002**, *23*(1), 79.
(22) Appleton, G. T.; Bennett, M. A.; Tomkins, I. B. *J. Chem. Soc., Dalton Trans.* **1976**, 439.
(23) Cooper, S. J.; Brown, M. P.; Puddephatt, R. J. *Inorg. Chem.* **1981**, *20*, 1374.
(24) Holtcamp, M. W.; Labinger, J. A.; Bercaw, J. E. *Inorg. Chim. Acta* **1997**, *265*, 117.

Table 1. Selected ^{1}H and ^{31}P{^{1}H} NMR Spectroscopic Data for Compounds Discussed in the Text[a]

			^{1}H NMR			^{31}P{^{1}H} NMR	
compd	*T*, K	solvent	δ(PtCH$_3$)	$^2J_{PtH}$	$^3J_{PH}$	δ	$^1J_{PtP}$
cis-[Pt(Me)$_2$(PEt$_3$)$_2$] (**1a**)	298	CD_2Cl_2	0.27	66.2	6.6	11.3	1858
cis-[Pt(Me)$_2$(PPr$^i_3$)$_2$] (**2a**)	298	CD_2Cl_2	0.31	66.9	6.3	33.7	1860
cis-[Pt(Me)$_2$(PCy$_3$)$_2$] (**3a**)	298	CD_2Cl_2	0.28	66.9	5.5	23.5	1824
cis-[Pt(Me)$_2$(P(4-MePh)$_3$)$_2$] (**4a**)	298	$CDCl_3$	0.37	69.2	7.1	26.1	1904
[Pt(Me)$_2$(dppm)] (**5a**)	298	$CDCl_3$	0.94	74.2	7.3	−38.8	1422
[Pt(Me)$_2$(dppe)] (**6a**)	298	$CDCl_3$	0.69	70.4	7.5	46.5	1782
[Pt(Me)$_2$(dppp)] (**7a**)	298	$CDCl_3$	0.33	68.6	5.7	3.5	1766
[Pt(Me)$_2$(dppb)] (**8a**)	298	$CDCl_3$	0.28	68.3	7.7	18.9	1847
cis-[Pt(Me)(Cl)(PEt$_3$)$_2$] (**1b**)	298	CD_2Cl_2	0.50	54.4	7.4	17.5	1737
						11.2	4225
cis-[Pt(Me)(Cl)(PPr$^i_3$)$_2$] (**2b**)	225	CD_3OD/CD_2Cl_2 (8/1 v/v)	0.58	53.2	7.0	32.8	1741
						27.6	4250
cis-[Pt(Me)(Cl)(PCy$_3$)$_2$] (**3b**)	225	CD_3OD/CD_2Cl_2 (8/1 v/v)	0.67	56.2	7.6	23.2	1753
						18.7	4328
cis-[Pt(Me)(Cl)(P(4-MePh)$_3$)$_2$] (**4b**)	298	$CDCl_3$	0.62	52.2	7.3	25.6	1775
						20.3	4450
[Pt(Me)(Cl)(dppm)] (**5b**)	298	CD_2Cl_2	0.72	62.0	8.9	−36.3	1248
						40.8	3876
[Pt(Me)(Cl)(dppe)] (**6b**)	298	$CDCl_3$	0.61	55.0	7.7	44.0	1725
						43.2	4264
[Pt(Me)(Cl)(dppp)] (**7b**)	298	$CDCl_3$	0.42	53.4	7.1	3.4	1654
						5.7	4178
[Pt(Me)(Cl)(dppb)] (**8b**)	298	$CDCl_3$	0.39	54.3	6.8	19.5	1711
						18.7	4385

[a] Resonances (δ) are in ppm and coupling constants $^2J_{PtH}$, $^3J_{PH}$ and $^1J_{PtP}$ in hertz.

Table 2. Selected ^{1}H NMR Spectroscopic Data for the Trans Monoalkyl Compounds 1c−4c and Related Pt(IV) Hydride Species[a]

	^{1}H NMR		
	δ(Pt−CH$_3$)[b]	δ(Pt−H)[c]	^{31}P{^{1}H} NMR δ[d]
trans-[Pt(Me)Cl(PEt$_3$)$_2$] (**1c**)	0.25 (84.0)		16.2 (2817)
[Pt(Me)Cl$_2$(H)(PEt$_3$)$_2$] (**1d**)	0.96 (62.5)	−18.8 (1228)	9.17 (1848)
trans-[Pt(Me)Cl(P(Pr$^i_3$)$_2$] (**2c**)	0.30 (83.4)		32.0 (2852)
[Pt(Me)Cl$_2$(H)(P(Pr$^i_3$)$_2$] (**2d**)	1.14 (57.1)	−17.4 (1362)	27.4 (2363)
2d′	1.14 (57.1)	−18.7 (1676)	29.0 (2785)
trans-[Pt(Me)Cl(PCy$_3$)$_2$] (**3c**)	0.20 (81.4)		21.0 (2821)
[Pt(Me)Cl$_2$(H)(PCy$_3$)$_2$] (**3d**)	0.81	−18.8 (1300)	
3d′	0.81	−17.6 (1354)	
trans-[Pt(Me)Cl(P(4-MePh)$_3$)$_2$] (**4c**)	−0.26 (79.6)		27.7 (3122)

[a] In CD_2Cl_2 at 220 K; resonances (δ) are in ppm. [b] $^2J_{PtH}$ values are reported in parentheses in hertz. [c] $^1J_{PtH}$ values are reported in parentheses in hertz. [d] $^1J_{PtP}$ values are reported in parentheses in hertz.

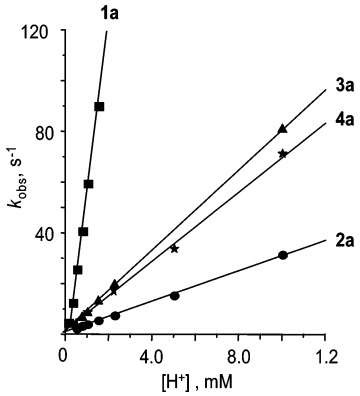

Figure 1. Dependence of the pseudo-first-order rate constants (k_{obs}/s^{-1}) on proton concentration for reactions of *cis*-[PtMe$_2$L$_2$] complexes (**1a**−**4a**, eq 2) in methanol at 298.2 K. For the sake of clarity the diagrams for compounds **5a**−**8a** have been omitted.

vs time data. The dependence of the pseudo-first-order rate constants (Table S2, in the Supporting Information) is described by a family of straight lines with zero intercept (Figure 1) and obeys eq 3.

$$k_{obs} = k_H[H^+] \quad (3)$$

Table 3. Second-Order Rate Constants, k_H and k_D, and Deuterium Kinetic Isotope Effects for the Protonolysis of the Platinum−Methyl Bond in the Complexes *cis*-[PtMe$_2$L$_2$] (1a−8a) and *cis*-[PtMeClL$_2$] (1b−8b)[a]

compd	L	k_H,[b] M^{-1} s^{-1}	k_D,[c] M^{-1} s^{-1}	k_H/k_D
1a	PEt$_3$	63400 ± 2150	24500 ± 300	2.59
2a	P(Pr^i)$_3$	3030 ± 30	1740 ± 10	1.74
3a	PCy$_3$	8050 ± 50	3090 ± 420	2.60
4a	P(4-MePh)$_3$	6960 ± 200	2610 ± 80	2.66
5a	$^1/_2$ dppm	30650 ± 1130	8730 ± 300	3.51
6a	$^1/_2$ dppe	30400 ± 1220	6420 ± 20	4.74
7a	$^1/_2$ dppp	25170 ± 340	5860 ± 470	4.30
8a	$^1/_2$ dppb	14900 ± 70	4230 ± 380	3.52
1b	PEt$_3$	1.068 ± 0.003	0.226 ± 0.005	4.73
2b	P(Pr^i)$_3$	0.0208 ± 0.0008	0.0153 ± 0.0005	1.36
3b	PCy$_3$	0.124 ± 0.001	0.0727 ± 0.0009	1.70
4b	P(4-MePh)$_3$	0.119 ± 0.004	0.0410 ± 0.0008	2.90
5b	$^1/_2$ dppm	0.129 ± 0.003	0.0751 ± 0.0006	1.72
6b	$^1/_2$ dppe	0.172 ± 0.006	0.0575 ± 0.0020	2.99
7b	$^1/_2$ dppp	0.195 ± 0.007	0.107 ± 0.005	1.82
8b	$^1/_2$ dppb	0.222 ± 0.013	0.0876 ± 0.0026	2.53

[a] At 298 K. [b] In CH_3OH. [c] In CH_3OD.

The values of k_H, from linear regression analysis of the dependence of k_{obs} on [H$^+$], are given in Table 3, together with their standard deviations. The values of k_H at different temperatures are set forth in Table S3 (Supporting Information), and

Table 4. Rate Constants and Activation Parameters for the Protonolysis of the Pt−Me Bond in *cis*-[PtMe$_2$L$_2$] Complexes[a]

compd	L	$10^{-4}k_H$ [b]	$\Delta H^{\ddagger}$ [c]	$\Delta S^{\ddagger}$ [d]
1a	PEt_3	6.34 ± 0.2	26.3 ± 1.0	−67 ± 4
2a	$P(Pr^i)_3$	0.30 ± 0.01	16.0 ± 0.5	−125 ± 2
3a	PCy_3	0.80 ± 0.01	36.1 ± 0.7	−49 ± 3
4a	$P(4\text{-MePh})_3$	0.69 ± 0.02	48.1 ± 2.4	−12 ± 8
5a	1/2 dppm	3.06 ± 0.1	35.7 ± 0.4	−43 ± 1
6a	1/2 dppe	3.04 ± 0.1	42.8 ± 0.7	−18 ± 2
7a	1/2 dppp	2.52 ± 0.03	35.7 ± 2.7	−44 ± 9
8a	1/2 dppb	1.49 ± 0.01	44.2 ± 5.3	−22 ± 18

[a] In methanol at 298 K. [b] In units of M^{-1} s^{-1}. [c] In units of kJ mol^{-1}. [d] In units of J K^{-1} mol^{-1}.

the associated activation parameters are given in Table 4. The same pattern of behavior is observed when the kinetic runs are carried out with DOTf and LiCl in CH_3OD, the only difference being a marked decrease of reactivity with respect to the protonolysis. The values of k_D derived from eq 4 are given in Table 3 together with the values of the calculated kinetic primary isotope effect.

$$k_{obs} = k_D[D^+] \tag{4}$$

Protonolysis of Monoalkyl *cis*-[PtMeClL$_2$] and [PtMeCl-(L-L)] Complexes. (a) NMR Measurements. Although all of the complexes **1b**−**8b** can be obtained easily "in situ" from the corresponding dialkyls, the NMR measurements were carried out using pure synthesized compounds as starting materials, except for **2b** and **3b**, which were prepared by acid attack from **2a** and **3a**, respectively. The cleavage of the Pt−C bond takes place according to the reaction

$$cis\text{-}[PtMeClL_2] \xrightarrow[[Cl^-]]{[H^+]} cis\text{-}[PtCl_2L_2] + CH_4 \tag{5}$$

The protonolysis rates appear to be many orders of magnitude slower than those of the corresponding dialkyls. As a consequence, in contrast to reaction 2, the process can be monitored by ^{1}H or ^{31}P NMR, modulating conveniently the reaction temperature and the concentration of added acid. This circumstance facilitated the search for the presence of possible platinum(IV) alkyl hydrido intermediates, performed by following the general procedure described in the Experimental Section. The ^{1}H and ^{31}P NMR spectra monitored soon after the treatment of **1b**−**8b** with HOTf and Ph_4AsCl, in CD_2Cl_2 at −78 °C correspond closely to that of the starting complexes. When the temperature is increased to −33 °C, even after 1 h there is no evidence for reactions or for the buildup of any intermediate species. At room temperature slow formation of *cis*-[PtCl$_2$L$_2$] and methane release can be monitored, except for **2b** and **3b**, which exhibit a concurrent geometrical isomerization leading to **2c** and **3c.** The same phenomena were observed in the reaction with DOTf in CD_3OD, with the only difference being the release of CH_3D instead of CH_4. When the reaction mixture was left at low temperature for a long time, no deuterium incorporation into the Pt−CH_3 site of unreacted *cis*-[PtMeClL$_2$] was observed.

(b) Spectrophotometric Studies. The spectral changes associated with eq 5 can be monitored through conventional spectrophotometry and exhibit well-defined isosbestic points. The systematic kinetics of these reactions were studied at various concentrations of H^+, D^+, and Cl^-. Once again, the reaction rates were independent of the concentration of Cl^-. The dependence of the pseudo-first-order rate constants on $[H^+]$ was consistent with eq 3 and that of $[D^+]$ with eq 4 (Table S4, in the Supporting Information). The values of k_H and k_D derived from eq 3 and eq 4, respectively, are given in Table 3 together with the values of the calculated kinetic isotope effect.

Chart 2. Structures of Stereoisomers Compatible with the ^{31}P{^{1}H} NMR Experimental Data for Pt(IV) Bis(phosphane) Dichloride Hydrido Alkyl Reaction Intermediates

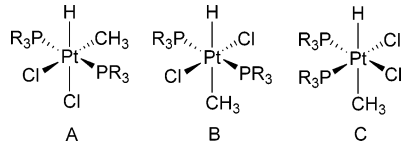

Protonolysis of Monoalkyl *trans*-[PtMeClL$_2$] Complexes. (a) NMR Measurements. Addition of an excess of HOTf (1/10, as a CD_2Cl_2 solution) to a solution of **1c** and Ph_4AsCl (1/10) in CD_2Cl_2 at −53 °C results in partial conversion to the oxidative addition product **1d**. The same treatment applied to **2c** and **3c** yields a pair of Pt(IV) compounds (**2d, 2d′** and **3d, 3d′**) for each starting material. Selected ^{1}H and ^{31}P resonances for all compounds are reported in Table 2**,** along with those of the starting Pt(II) complexes. When the temperature is raised, reductive elimination of methane takes place, accompanied by the formation of *trans*-[PtCl$_2$L$_2$]. Protonation of **1c**−**3c** with DOTf in CD_3OD results in deuterium incorporation into the coordinated methyl site prior to CH_3D, CH_2D_2, and CHD_3 loss, which implies the presence of unstable Pt^{IV}(D)Me intermediates not detected by ^{1}H and ^{31}P NMR. These results were not unexpected, in light of similar previous findings on **1c** and on *trans*-[PtMeBr(PEt$_3$)$_2$], *trans*-[PtEtCl(PEt$_3$)$_2$], and *trans*-[PtBzCl-(PEt$_3$)$_2$] by Bercaw et al.,[12,24] which have been explained by (i) oxidative addition of HCl to the planar substrate and (ii) isotopic exchange on Pt^{IV}Me(D) through the intermediacy of a four-coordinate σ-alkane complex.

(b) Stereochemistry of HCl Addition. For [PtMeCl$_2$(H)-(PEt$_3$)$_2$] (**1d**) the characteristic Pt−H resonance appears far upfield (δ −18.8 ppm) with the corresponding platinum satellites ($^1J_{PtH}$ = 1228 Hz). The Pt−Me resonance moves downfield with respect to that of **1c** (δ 0.96 ppm), showing a lower value for the ^{195}Pt satellite signal ($^2J_{PtH}$ = 63 Hz). These data correspond closely to those reported by Bercaw et al. for [PtMeCl$_2$(H)-(PEt$_3$)$_2$].[12] The theory predicts six possible stereoisomers for an octahedral species of the type Ma$_2$b$_2$cd. Only three of them are compatible with a single ^{31}P resonance for two magnetically equivalent phosphorus atoms (Chart 2).

A large value of the $^1J_{PtH}$ coupling constant is considered diagnostic for a hydride trans to a weakly trans-activating group (Cl) rather than to a strong σ-donor methyl ligand.[7] In addition, the magnitudes of the coupling constants $^1J_{PtP}$ are consistent with mutual trans positions of the two phosphanes.[25] Thus, structure A would be preferred over structures B and C for **1d**. This stereochemical arrangement should be the result of trans addition of HCl to **1c**. By analogy, structure A should be associated with the product formed on protonation of **2c** and **3c**. The observation of two oxidation products, each characterized by a single ^{31}P resonance and large values of $^1J_{PtP}$, could be tentatively explained by the concurrent formation of species having the solvent or OTf^- in the position trans to the hydride together with the chloride [PtMeCl$_2$(H)(PPr$^i_3$)$_2$] and [PtMeCl$_2$-(H)(PCy$_3$)$_2$] species.

(25) (a) Anderson, D. W. W.; Ebsworth, E. A. V.; Rankin, D. W. H. *J. Chem. Soc., Dalton Trans.* **1973**, 854. (b) Blacklaws, I. M.; Brown, L. C.; Ebsworth, E. A. V.; Reed, F. J. S. *J. Chem. Soc., Dalton Trans.* **1978**, 877.

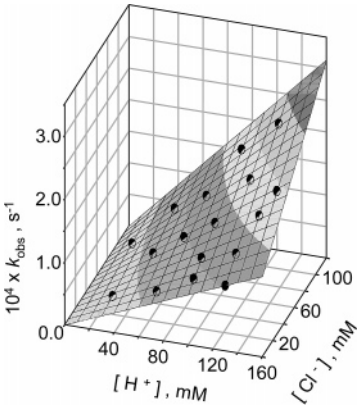

Figure 2. 3D plot showing the dependence of the observed pseudo-first-order rate constants (k_{obs}/s^{-1}) for reactions of *trans*-[PtMeCl(PEt$_3$)$_2$] as a function of the proton and chloride ion concentrations in methanol at 298 K.

Table 5. Second-Order Rate Constants, k_H and k_D, and Deuterium Kinetic Isotope Effects for the Protonolysis of the Platinum−Methyl Bond in the Complexes *trans*-[PtMeClL$_2$] (1c−4c)[a]

compd	L	10^3k_H,[b] M^{-1} s^{-1}	10^3k_{Cl},[b] M^{-2} s^{-1}	10^3k_D,[c] M^{-1} s^{-1}	$10^3k'_{Cl}$,[c] M^{-2} s^{-1}	k_H/k_D
1c	PEt_3	2.08 ± 0.3	326 ± 6	3.46 ± 0.5	413 ± 6	0.60
2c	$P(Pr^i)_3$	0.29 ± 0.01	0.52 ± 0.04	0.74 ± 0.04	2.62 ± 0.6	0.39
3c	PCy_3	0.81 ± 0.02	9.4 ± 0.4	2.14 ± 0.04	26.7 ± 1	0.38
4c	P(4-MePh)$_3$	1.92 ± 0.1	116 ± 2	2.77 ± 0.2	110 ± 3	0.69

[a] At 298 K. [b] In CH_3OH. [c] In CH_3OD.

(c) Spectrophotometric Studies. Protonolysis of *trans*-[PtMeClL$_2$] complexes has been the subject of several kinetic studies in the past, particularly as far as compound **1c** is concerned.[6a,i,12] As in previous investigations, we utilized UV−visible spectroscopy to monitor these reactions, which take place smoothly and quantitatively according to eq 6.

$$\textit{trans}\text{-}[PtMeClL_2] \xrightarrow[[Cl^-]]{[H^+]} \textit{trans}\text{-}[PtCl_2L_2] + CH_4 \qquad (6)$$

Several clean isosbestic points characterize the spectral changes. Obviously, the Pt(IV) intermediates responsible for deuterium exchange into the methyl sites in CD_3OD (see above) cannot be seen in the electronic spectrum. The systematic kinetics of these reactions were studied at different proton and chloride concentrations, and the calculated values of the pseudo-first-order rate constants k_{obs} are available in the Supporting Information (Table S5). The dependence of the rates on $[H^+]$, at constant chloride concentration, is represented by a straight line passing through the origin. At constant proton concentration the rates were linearly dependent on $[Cl^-]$ (with a nonzero intercept). A global 3-D representation of the $[H^+]$ and $[Cl^-]$ dependence of the kinetic data for the protonolysis of **1c** is given in Figure 2.

All of the rate data appear to fit the rate law

$$k_{obs} = k_H[H^+] + k_{Cl}[H^+][Cl^-] \qquad (7)$$

which includes a chloride-dependent term. The values of k_{obs}, $[H^+]$, and $[Cl^-]$ were fitted to this expression by using a multiple-linear nonweighted regression. The best values of the constants k_H and k_{Cl} are given in Table 5, together with their standard deviations. The kinetic runs with DOTf in CH_3OD were carried out over a range of $[D^+]$ and $[Cl^-]$ concentrations, and the values of k_D and k'_{Cl} derived from eq 8 are given in Table 5 together with the values of the calculated kinetic primary isotope effect.

$$k_{obs} = k_D[D^+] + k'_{Cl}[D^+][Cl^-] \qquad (8)$$

Discussion

The synthesis of the complexes **1a**−**8a**, **1b**−**8b**, and **1c**−**4c** has been performed by adopting slight modifications to well-established procedures. The various steps (Scheme 2) involve the use of *cis*-[PtMe$_2$(Me$_2$SO)$_2$] as a precursor in the synthesis of **1a**−**8a** and of *trans*-[PtMeCl(Me$_2$SO)$_2$] as a precursor in the synthesis of **1c**−**4c** and a series of protonolysis reactions.

Problems arise only when using sterically demanding phosphanes such as PPr^i_3 and PCy_3. With such ligands, the substitution reaction at *cis*-[PtMe$_2$(Me$_2$SO)$_2$] often does not go to completion, giving a mixture of mono- and bis-substituted cis products. In addition, protonolysis of both *cis*-[PtMe$_2$(PPr^i_3)$_2$] (**2a**) and *cis*-[PtMe$_2$(PCy_3)$_2$] (**3a**) with HCl at room temperature gives directly the trans monochloride derivatives **2c** and **3c**, as a result of a well-known spontaneous geometrical isomerization of cis monoalkyl halide compounds[13,15] that is accelerated by the encumbrance of the phosphane ligand.[21] In any case, the product formed upon electrophilic attack by the proton maintains the stereochemistry of the starting complex. A preliminary search for the buildup of Pt(IV) intermediates species upon protonation of the substrate in CD_2Cl_2 and/or H/D exchange and deuterium incorporation in the reagents and products in CD_3OD has been carried out systematically for all compounds by NMR at low temperature. In methanol, at room temperature, ^1H and ^{31}P NMR and UV/vis spectral changes of these reactions always showed the presence of only two species, the starting complex and the final product.

Kinetic Features of *trans*-[Pt(R)XL$_2$] Complexes. Several studies have provided a detailed understanding of the mechanism of protonation of *trans*-[PtMeCl(PEt$_3$)$_2$] (**1c**). A two-step S_E(ox) mechanism was originally proposed by Belluco et al,[6a] based essentially on the form of the rate law equation, which includes a chloride-dependent term and the chemical evidence for easy access to the Pt(IV) oxidation state. Interestingly, new findings by Bercaw[12,24] were consistent with the metal being the kinetically preferred site of protonation and ruled out the alternative mechanism of protonation at the methyl group. Indeed, several factors such as (i) observation of [PtMeCl$_2$(H)-

Scheme 2. Synthesis of Platinum(II) Complexes

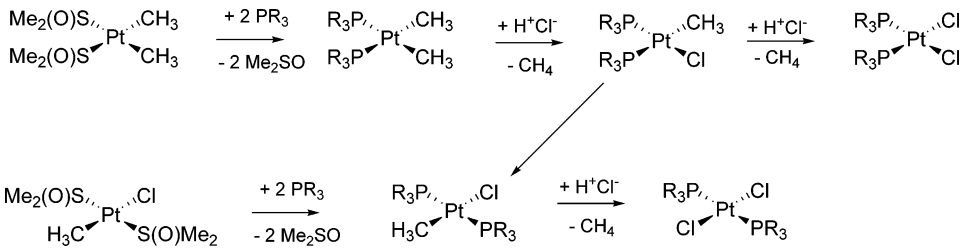

Scheme 3. Currently Accepted Oxidative-Addition−Reductive-Elimination Mechanism

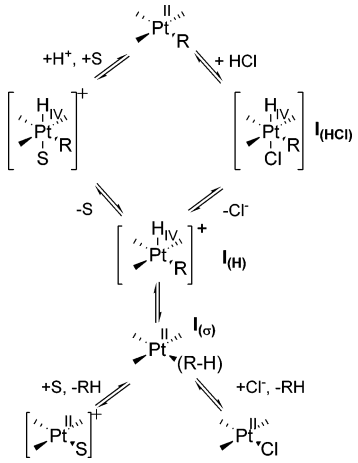

$(PEt_3)_2$] at −78 °C in CD_2Cl_2, (ii) the kinetics of its reductive elimination, and (iii) multiple D incorporation into unreacted Pt−CH_3 with concurrent loss of CH_nD_{n-4} isotopomers in methanol all concur with a verification and refinement of the original reaction scheme that currently include (Scheme 3) the intermediacy of a square-pyramidal five-coordinate Pt(IV) hydride ($I_{(H)}$ in Scheme 3) and the formation of an elusive σ-alkane complex ($I_{(\sigma)}$ in Scheme 3).

The results of this work confirm and extend to complexes **2c** and **3c** some fundamental features exhibited by protonolysis reactions of **1c** such as (i) the form of the rate law, (ii) the buildup of Pt(IV) hydride intermediates on protonation of the substrates in dichloromethane, and (iii) the evidence for H/D scrambling in methanol prior to methane loss and subsequent observation of the CH_nD_{4-n} isotopomers. Thus, we can confidently assume that the S_E(ox) mechanism in Scheme 3 applies to complexes **1c**−**4c** and to closely related species. Figure 3 shows a qualitative energy profile based on Scheme 3 that accounts for the kinetic features exhibited by the protonolysis of *trans*-[PtMeClL_2] complexes *in methanol*. The rate-determining step is loss of alkane from the σ-complex.

Examination of the rate data in Table 5 adds a number of significant observations to the mechanistic picture. The measurement of the solvent kinetic isotope effect (KIE) reveals that this multistep pathway is characterized by *inverse* KIE values ($k_H/k_D < 1$), as expected for a sequence of proton-transfer equilibria followed by a rate-determining reaction of the protonated substrate. Similar KIE's have been observed in many cases of reductive elimination from alkyl hydride and alkyl deuteride complexes[26] and were interpreted in terms of the inverse equilibrium isotope effect $K_{e,H}/K_{e,D} < 1$, which controls C−H(D) bond formation in the intermediate σ-alkane complex (the passage from $I_{(H)}$ to $I_{(\sigma)}$ in the coordinate reaction diagram), combined with comparable values for the rates of hydrocarbon dissociation from M(R−H) and M(R−D). Interestingly, the contributions of the chloride-dependent pathways, indicated by the values of the third-order rate constants k_{Cl} and k'_{Cl}, are comparable but not identical for protonolysis and deuteriolysis on the same substrate. This contribution is significant compared to that of k_H or k_D in the unhindered complexes **1c** and **4c** but is likely to vanish when the steric hindrance is increased at the central metal, as shown by the rate data for **2c** and **3c**. This variability of the importance of the chloride-dependent term with the steric hindrance of the substrates is a further indication that the form of the rate law can hardly be assumed as a clear-cut diagnostic tool in assessing the reaction mechanism. The bulk at the metal site plays a much less marked role in controlling the protonation rates k_H or k_D along the series of examined complexes **1c**−**4c**. The number of data points is insufficient to perform a statistically satisfactory quantitative analysis of ligand effects (QALE)[27] on the reactivity, but it is clear that protonation at the metal is favored by a transfer of electronic density from the ligand to the metal and is impeded by steric congestion.

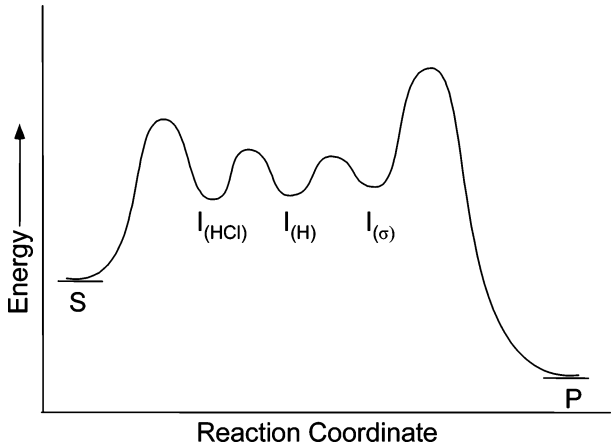

Figure 3. Qualitative reaction coordinate diagram (based on Scheme 3) for the protonolysis reactions of *trans*-[Pt(R)Cl$(PR_3)_2$] complexes in methanol. S represents the starting complex, $I_{(HCl)}$, $I_{(H)}$, and $I_{(\sigma)}$ the transient intermediates [Pt(R)Cl_2(H)$(PR_3)_2$], [Pt(R)Cl(H)$(PR_3)_2$]$^+$, and [PtCl$(PR_3)_2$(σ-RH)], respectively, and P the reaction product.

An important question pertaining to these protonation reactions is the extent to which a change in coordinative environment can promote a change of mechanism and of site attack. A survey of literature data for closely related compounds can shed some light on this matter. A change in the organic moiety along the series of complexes *trans*-[Pt(R)Cl$(PEt_3)_2$] (R = Et, *n*-Pr, *n*-Bu, benzyl)[6i] does not apparently produce any change with respect to the kinetic features observed for **1c**−**4c**: (i) same rate law and (ii) sequence of reactivity for k_H, Et > *n*-Pr > *n*-Bu > Me > benzyl, which parallels the rate of deuterium incorporation into the α-position of the alkyl group in CD_3OD/DOTf, Et > Me > benzyl.[24] The mechanistic picture changes markedly on increasing the trans-activating effect of X in *trans*-[PtMe(X)$(PEt_3)_2$] complexes. When X = Br^-, a bivariate rate law[6a] and multiple H/D exchange[24] are still observed. With X = I^-, the halide-dependent term vanishes[6a] and only monodeuterated methane is observed on deuteriolysis.[24] Introducing in the system a strong σ-donor carbon ligand R (R = *o*-, *m*-, and *p*-substituted aryl ring)[6e] the proton attack occurs selectively at the methyl group, with the simplified rate law $k_{obs} = k_H[H^+]$ and an increase of reactivity of about 7 orders of magnitude with respect to that of the chloride analogue (k_H(Ph)/k_H(Cl) = 20 300/0.002 = 1.01×10^7). In addition, deuteriolysis leads to the formation of only CH_3D and, most importantly, the KIE is strongly *positive* ($k_H/k_D \approx 7$). All of these findings are consistent with a rate-determining proton transfer to the substrate, whatever the site of the proton attack is, and will be discussed in connection with other results obtained in this work. A recent report by Puddephatt et al.[28] on the protonolysis of phenyl−platinum(II) bonds in [PtPh(NCN)] (NCN = 2,6-$C_6H_3(CH_2NMe_2)_2$), a complex with

(26) Jones, W. D. *Acc. Chem. Res*. **2003**, *36*, 140−146.

(27) http://www.bu.edu/qale. This Web site collects sets of data, protocol for the analysis, program package, parameters of ligands, leading references, etc. Each set of data, taken from the literature, is subjected to a QALE analysis with commentary on how each analysis is done and how successful it is. All of the material is updated with recent data sets and analyses.

a phenyl trans to a carbon donor, seems to be in contrast with what is expected for complexes having mutually trans Pt−C-bonded groups, because of the unambiguous disposition showed by the complex to an oxidative−reductive behavior. However, it is possible that the π-bonding system of the in-plane aryl ring of the cyclometalated NCN ligand in [PtPh(NCN)] is able to relieve the excess electron donation by the trans phenyl ligand, promoting kinetic features similar to those of [$PtMe_2$(N-N)] complexes.

Kinetic Features of *cis*-[Pt(R)XL$_2$] Complexes. In the systems analyzed in this study (R = Me, X = Cl; L = PEt_3, $P(Pr^i)_3$, PCy_3, $P(4\text{-MePh})_3$, **1b**−**4b**; L-L = dppm, dppe, dppp, dppb, **5b**−**8b**) the trans-activating groups are phosphanes of widely different steric and electronic characteristics with chelate rings of increasing size. The rate law is $k_{obs} = k_H[H^+]$, and the halide ion has no influence on the rate. No Pt(IV) intermediates are detected, nor is deuterium incorporation into the coordinated methyl observed. No methane isotopomers different from CH_3D are observed, as reported before for *cis*-[PtMeCl($(MeO)_3P)_2$].[24] Interestingly, the KIE's are *positive* in all cases, with a mean value of 2.5 ± 1. None of the diagnostic tools that supported the S_E(ox) mechanism for the corresponding trans analogues are readily available. Rather, these results are strongly in favor of a rate-determining proton transfer to the substrate, whatever the site of the proton attack is.

The nature of the P-donor ligands L significantly affects the rates (see data in Table 3). The efficiency of the spectator P-donor ligands in accelerating the proton attack increases in the order $P(Pr^i)_3 < P(4\text{-}MeC_6H_4)_3 \approx PCy_3 < PEt_3$, the difference in reactivity between the first and the last members of the series being about 1 order of magnitude. The sequence of reactivity reflects the extent of steric congestion or electron donation by the P-donor ligands. The rate of methane loss on protonation is at least 100 times higher for the complexes *cis*-[PtMeCl($PR_3)_2$] (**1b**−**4b**) than for the corresponding trans complexes (**1c**−**4c**). The ring size does not appear to have a significant effect on the rates of protonation and deuteriolysis (cf. **5b**−**8b**). More electrophilic Pt centers, such as [PtMeX(dfpe)] (dfepe = $(C_2F_5)_2$-$PCH_2CH_2P(C_2F_5)_2$; X = O_2CCF_3, OSO_2H, OSO_2CF_3, OSO_2F) complexes, are much more resistant to protonolysis, requiring prolonged reaction times and heating in the neat solvents.[29] The absence of kinetic dependence on chloride concentration, the absence of Pt(IV) intermediates by variable-temperature NMR in dichloromethane, and positive KIE values were observed in this study. In contrast, *trans*-[PtMeX($PMe(C_2F_5)_2)_2$] complexes show a significant tendency toward deuterium incorporation into the Pt−methyl group.[17] Thus, apart from a remarkable difference of reactivity, the (fluoroalkyl)phosphane systems show a clear analogy of kinetic behavior with the corresponding alkylphosphanes, with a propensity of trans isomers (Cl trans to CH_3) toward an S_E(ox) mechanism and of the cis isomers (phosphane trans to CH_3) toward an S_E2 mechanism.

Kinetic Features of *cis*-[Pt(R)(R′)L$_2$] Complexes. The systems analyzed in this study were those in which R = R′ = Me and L = PEt_3, $P(Pr^i)_3$, PCy_3, $P(4\text{-MePh})_3$ (**1a**−**4a**) and L-L = dppm, dppe, dppp, dppb (**5a**−**8a**). The rate law is $k_{obs} = k_H[H^+]$, and no kinetic influence of the chloride ion was observed. The search for Pt(IV) intermediates by low-temperature NMR in dichloromethane was unsuccessful, as was the search for deuterium incorporation into the Pt−methyl group. Interestingly, treatment of [$PtMe_2$(depe)] with DOTf in CD_3OD at −70 °C was reported to result in the immediate formation of CH_3D and a monomethyl solvento species.[24] Deuteriolysis of **1a**−**8a** leads to the formation of only CH_3D, and the KIE values are always *positive*, with a mean value of 3.2 ± 1. The reactions are characterized by low values of activation enthalpy and highly negative values of activation entropy. At this stage it is worth recalling that negative volumes of activation are associated with the protonolysis of the parent complexes *cis*-[$PtR_2(PEt_3)_2$] (R = linear or branched alkyl groups) and *cis*-[Pt(R)(R′)$(PEt_3)_2$] (R′ = Me). As for the compounds **5b**−**8b**, chelation and ring size do not affect significantly the reactivity of compounds **5a**−**8a**.

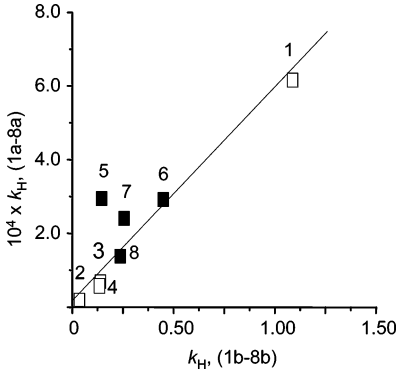

Figure 4. Correlation between the second-order rate constants k_H (M^{-1} s^{-1}) for protonolysis of the dialkyl complexes *cis*-[$PtMe_2L_2$] (**1a**−**8a**) and related monoalkyl compounds *cis*-[PtMeClL_2] (**1b**−**8b**) in methanol at 298 K. Numbers refer to compounds as listed in Table 3.

The series of trans-activating effects by the P-donor in determining the rate of proton attack is the same as that for compounds **1b**−**8b**. Moreover, a straight line correlates the two series of second-order rate constants values k_H (Figure 4).

Linear regression analysis of this plot gives the equation $k_H(Pt_{Me_2}) = (1780 \pm 1180) + (57900 \pm 2400)[k_H(Pt_{MeCl})]$. Thus, the rate of methane loss on protonation of **1a**−**8a** is about 5 orders of magnitude higher than that for the corresponding *cis*-monoalkyl chloride compounds. Deviation from linearity in the plot, observed for some data points pertaining to chelate complexes, can be explained by differences in torsion angles between dialkyls and monoalkyl compounds having the same ring size (especially in the case of **5a** and **5b**, with dppe as chelating ligand).

A marked difference in rates of protonolysis was already measured between the complexes [$PtMe_2$(dfepe)] and [PtMeCl-(dfepe)] and was interpreted by a possible diversity of reaction mechanism dictated by the wide difference in electron densities at the metals of the two complexes.[29]

Apart from the extreme similarity of the kinetic features, the good linear correlation in Figure 4 rules out this possibility for dialkyl complexes **1a**−**8a** and monoalkyl complexes **1b**−**8b** and strongly indicates a common mechanism. This is confirmed by the very similar KIE values measured for the attack at the first and at the second methyl group. All the kinetic evidence in the two cases militates against a multistep mechanism and is in favor of a direct proton transfer in the transition state.

Primary Attack at Metal or Ligand? In this work we have evaluated the kinetic features for electrophilic attack by the proton on three systems, (i) *cis*-[$PtMe_2L_2$], (ii) *cis*-[PtMeClL_2], and (iii) *trans*-[PtMeClL_2], through a variety of kinetic and NMR measurements and have examined their correspondence with literature data for closely related compounds. In an attempt to

(28) Ong, C. M.; Jennings, M. C.; Puddephatt, R. J. *Can. J. Chem.* **2003**, *81*, 1196.

(29) Bennett, B. L.; Hoerter, J. M.; Houlis, J. F.; Roddick, D. M. *Organometallics* **2000**, *19*, 615.

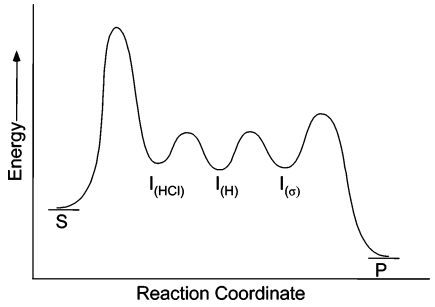

Figure 5. Qualitative coordinate reaction diagram for a rate-determining initial protonation in an $S_E(ox)$ mechanism. The symbols S, $I_{(HCl)}$, $I_{(H)}$, and $I_{(\sigma)}$ and P have the same meaning as in Figure 3.

rationalize the diverse kinetic results within a unified picture, indirect arguments can never be completely conclusive. For example, we can hardly rely on the form of the kinetic rate law or on the analysis of steric or inductive effects of substituents on the ligands. Thus, electron release should increase and steric congestion should decrease the rate in either a $S_E(ox)$ or S_E2 reaction pathway. Much more reliable diagnostic tools are the detection of transient intermediates and/or the magnitude and sign of kinetic parameters (such as entropies of activation, volumes of activation, and isotope effects), which are indicative of the extent of proton involvement in the transition state. From these criteria two different categories of reactions can be distinguished: (i) those involving a rate-determining proton transfer to the substrate (either to the Pt−C σ-bond or to the metal) and (ii) multistep reactions, where the important target of detecting a hydride intermediate with an intact Pt−C bond can be achieved. Protonolyses on *cis*-[$PtMe_2L_2$] and *cis*-[$PtMeClL_2$] belong to the first category, as presumed by the lack of direct or inferred evidence of Pt(IV) intermediates, by the largely negative values of entropies and volumes of activation, and by the *positive* values of KIE. In contrast, the kinetic features of the third system (trans derivatives), which is simply a different geometrical shape of the second, are perfectly in keeping with a multistep $S_E(ox)$ mechanism, as suggested by the intermediacy of Pt(IV) species and by *inverse* values of KIEs.

We are inclined to think that the geometry of the compounds hardly plays a significant role in determining such kinetic differences. Rather, the nature of the group in the position trans to the Pt−C bond is crucial. If we agree to the intermediacy of platinum(IV) hydrido species as a general rule for protonolysis of the metal−carbon bond for electron-rich alkyl complexes of platinum(II), the explanation that could be offered, according to the $S_E(ox)$ mechanism, is that the nature of the trans ligand markedly affects the relative energies and stabilization of the intermediates $I_{(HCl)}$, $I_{(H)}$, and $I_{(\sigma)}$ in the energy profile of Figure 3. When the trans effect is increased along the series $Cl^- < Br^- < I^- < PR_3 <$ C(alkyl), the qualitative form of the reaction coordinate diagram changes from that in Figure 3 to that in Figure 5.

As a result, the mechanism must entail a rate-determining oxidative-addition reaction, with undetectable small concentrations of oxidized intermediate. This qualitative coordinate reaction diagram is consistent also with a very fast extrusion of the alkane from the σ-alkane complex $I_{(\sigma)}$ upon nucleophilic attack by the nucleophile (halide ion or solvent), the lack of multiple H/D exchange, and the formation of only CH_3D upon deuteriolysis.

A reasonable alternative is that strong electron donation from the trans-activating group promotes an increase of electron

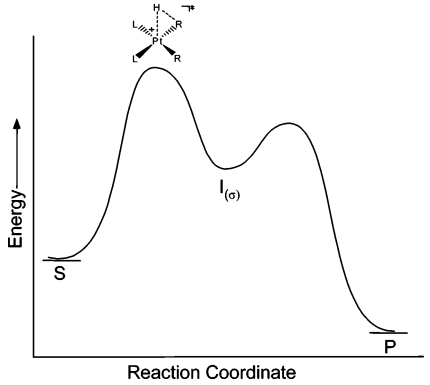

Figure 6. Qualitative coordinate reaction diagram for a rate-determining proton attack at the Pt−C σ-bond of S with release of alkane in a three-center transition state (S_E2 mechanism).

Scheme 4. Three-Center−Two-Electron Transition State in the Formation of the σ-Alkane Complex

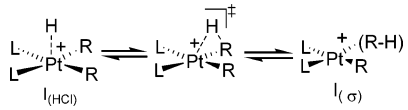

density at the Pt−alkyl σ-bond of the four-coordinate starting complex, combined with a significant $L_nPt^{\delta+}-C^{\delta-}$ bond polarization. As a consequence, either the carbon atom or the Pt−alkyl σ-bond become the favored sites of protonation. If the synchronous attack takes place at the Pt−C σ-bond, the energy profile has the form illustrated in Figure 6, where the point of highest energy is a three-center transition state in which there is extensive involvement of the proton, considerable stretching of the Pt−C bond, and no assistance by halide ions. This could still be the most likely pathway if the Pt−C σ bond is the highest occupied molecular orbital.[6g]

In conclusion, the similarity of the energy profiles in Figures 5 and 6, both describing the coordinate reaction for a rate-determining proton transfer to the substrate, suggests that, under these circumstances, any discussion of the site of proton attack risks becoming semantic in nature. This is still more understandable if one considers that a three-center−two-electron species could well be found along the path toward the formation of the σ-alkane complex from the platinum(IV) hydrido alkyl intermediate in an $S_E(ox)$ process (Scheme 4).

We can conclude that (i) isotopic scrambling and detection of platinum(IV) alkyl hydrido intermediates are the most definitive evidence for the oxidative-addition mechanism in complexes of the type [$PtMe_2$(N-N)], [PtMeCl(N-N)], and *trans*-[$PtMeX(PR_3)_2$] (X = Cl, Br) and (ii) when the trans-labilizing effect of donor atoms is increased along the series $I^- < PR_3 <$ C(alkyl), the initial protonation becomes the rate-determining step and it is difficult or impossible to identify the site of attack and decide whether a $S_E(ox)$ mechanism is still operating or an S_E2 mechanism has taken over.

Relevance to C−H Bond Activation. The role of platinum(IV) hydrido intermediates is well-established in the protonolysis of [$PtMe_2$(N-N)] complexes[11] and in the microscopic reverse activation of alkanes or arenes by the related cationic compounds $[PtMe(N\text{-}N)(S)]^+$ (S = weakly coordinating solvent).[14] A result of this work is that full oxidation of the metal is not a prerequisite for all protonolysis reactions and there is no reason to assume, "by analogy", $S_E(ox)$ as a general mechanism for electrophilic breakage of the Pt−C bond. In contrast to the expectation of a facile oxidation of platinum(II) electron-rich complexes, it was shown that the possibility of "one-step"

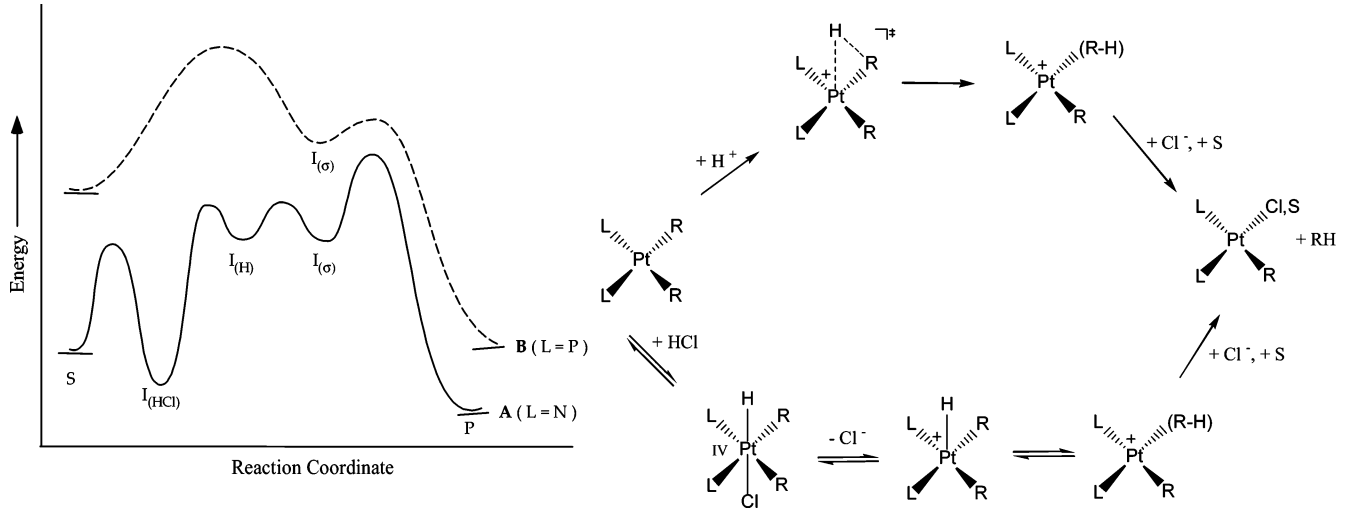

Figure 7. Comparison of qualitative coordinate reaction diagrams for electrophilic attack by the proton at a platinum−alkyl substrate occurring with an $S_E(ox)$ mechanism (**A**) or with an S_E2 mechanism (**B**).

electrophilic attack at the Pt−C bond increases with increasing electron donation brought about by the trans ligand. The probability of intercepting Pt(IV) hydrido alkyl intermediates along the energy profile decreases. The reason for this seems to be a preferential electron enrichment and increase of energy at the Pt−C σ-bond combined with a significant $LnM^{\delta+}-C^{\delta-}$ bond polarization. Thus, the Pt−C bond becomes the preferential site of attack in a one-step transfer of the proton characterized by a three-center transition state. In addition, a strong donor makes the complex more susceptible to protonation. Apart from the kinetic data discussed above, a number of examples in the literature prove this assumption. Interestingly, a comparison of the kinetic behavior between *trans*-[Pt(Ph)(Me)$(PEt_3)_2$] and *trans*-[PtCl(Me)$(PEt_3)_2$] is paradigmatic for a concurrent change of site attack (Pt−C vs Pt) and of increase of reactivity (7 orders of magnitude on going from Cl to Ph).

In light of the kinetic results of this work, there is sufficient reason to consider a phosphane as a strongly trans-activating ligand promoting an S_E2 mechanism. Thus, it is of interest to evaluate the effect of the change from N- to P-donor ligands, because a choice of ligands has a great effect on the efficiency of C−H activation at Pt(II) centers. The situation is summarized in simplified form in Figure 7, which illustrates in terms of qualitative reaction coordinate diagrams the chemical characteristics of two systems containing nitrogen (**A**) or phosphorus donor atoms (**B**) as trans ligands, respectively. The scheme is also consistent with the general view that N-based ligands are able to stabilize the Pt(IV) oxidation state better than P-based ligands.[30] Looking at the two plots in Figure 7 from the right to the left side can help in drawing some conclusions on the relative efficiency of platinum(II) phosphane or diimine complexes in activating C−H bonds.[31]

The two strong donor phosphane ligands in **B** will markedly affect the rate of ligand substitution. Under a strong trans-activating effect, the alkane will enter the coordination sphere of the metal more easily in **B** than in **A**. Likewise, the activation energy for alkane loss from the σ-alkane complex will be much lower in **B** than in **A**, whatever the details of this reaction step (dissociative or associative). The facile access of the alkane (or arene) to the coordination sphere of the metal in **B** is balanced by its much easier removal, the rate-determining step shifts to the actual C−H bond activation, and the overall energetics will be less favorable in **B** than in **A**. A similar analysis was performed by Puddephatt on the qualitative energy profiles of two $S_E(ox)$ processes to predict the efficiency in activating the arene C−H bond by [PtX(NCN)], a cyclometalated complex characterized by a strong trans activating carbon atom, as compared to the parent [PtPhX(NN)] complex.[28]

The good efficiency of Pt(II) bis(N-donor) alkyl complexes in activating the C−H bond is reflected in the rapidly growing number of examples that can be found in the literature for these reactions.[14] Relatively fewer cases refer to Pt(II) phosphane alkyl complexes.[32] However, several examples of intramolecular C−H bond activation of phosphane ligands have been reported for cycloplatination reactions.[33] Cases in which cyclometalation is initiated by ligand dissociation followed by an agostic interaction of the resulting three-coordinate T-shaped 14-electron intermediate with the σ(C−H) orbital of a methyl group have been recently reported.[34] The exact mechanism for these C−H bond-cleavage reactions is still unknown and deserves further study because of its strong connection with the design of a model for the still elusive platinum(II) σ-alkane complexes.

Experimental Section

General Procedures and Chemicals. All syntheses were performed on a double-manifold Schlenk vacuum line under a dry

(30) (a) Hill, G. S.; Puddephatt, R. J. *Organometallics* **1998**, *17*, 1478. (b) Rendina, L. M.; Puddephatt, R. J. *Chem. Rev.* **1997**, *97*, 1735. (c) van Asselt, R.; Rijnberg, E.; Elsevier, C. J. *Organometallics* **1994**, *13*, 706.

(31) The position of the two profiles with respect to one another is completely arbitrary, and therefore, no quantitative comparison should be made between the energies of the various species (P vs N). Only the relative barrier heights at each (separate) profile are significant.

(32) (a) Brainard, R. L.; Nutt, W. R.; Lee, T. R.; Whitesides, G. M. *Organometallics* **1988**, *7*, 2379. (b) Konze, W. V.; Scott, B. L.; Kubas, G. J. *J. Am. Chem. Soc.* **2002**, *124*, 12550. (c) Peters, R. G.; White, S.; Roddick, D. M. *Organometallics* **1998**, *17*, 4493.

(33) (a) Fornies, J.; Martin, A.; Navarro, R.; Sicilia, V.; Villarroya, P. *Organometallics* **1996**, *15*, 1826. (b) Chappell, S. D.; Cole-Hamilton, D. J. *J. Chem. Soc., Dalton Trans.* **1983**, 1051. (c) Cheney, A. J.; Shaw, B. L. *J. Chem. Soc., Dalton Trans.* **1972**, 754. (d) Thorn, D. L. *Organometallics* **1998**, *17*, 348. (e) Alyea, E. C.; Ferguson, G.; Malito, J.; Ruhl, B. L. *Organometallics* **1989**, *8*, 1188. (f) Alyea, E. C.; Malito, J. *J. Organomet. Chem.* **1988**, *340*, 119. (g) Scheffknecht, C.; Rhomberg, A.; Müeller, E. P.; Peringer, P. *J. Organomet. Chem.* **1993**, *463*, 245. (h) Clark, H. C.; Goel, A. B.; Goel, R. G.; Goel, S. *Inorg. Chem.* **1980**, *19*, 3220.

(34) (a) Plutino, M. R.; Monsù Scolaro, L.; Albinati, A.; Romeo, R. *J. Am. Chem. Soc.* **2004**, *126*, 6470. (b) Plutino, M. R.; Romeo, R.; Romeo, A. *Helv. Chim. Acta* **2005**, *88*, 507. (c) Baratta, W.; Stoccoro, S.; Doppiu, A.; Herdtweck, E.; Zucca, A.; Rigo, P. *Angew. Chem., Int. Ed.* **2003**, *42*, 105. (d) Ingleson, M. J.; Mahon, M. F.; Weller, A. S. *Chem. Commun.* **2004**, 2398.

and oxygen-free dinitrogen atmosphere using freshly distilled, dried, and degassed solvents. Solvents employed in the synthetic procedures (Analytical Reagent Grade, Lab-Scan, Ltd.) were distilled under dinitrogen from sodium−benzophenone ketyl (tetrahydrofuran, diethyl ether, toluene) or barium oxide (dichloromethane).[35] Spectrophotometric grade methanol, phosphane ligands, HCF_3SO_3, DCF_3SO_3, Chloroform-*d* (99.8+%, CIL, Inc.), toluene-d_8 (99+%), CH_3OD, and CD_3OD were purchased from Aldrich Chemical Co. and used as received. Elemental analyses were performed by the Microanalytical Laboratory, Department of Chemistry, University College Dublin, Belfield, Dublin 4, Ireland.

Instrumentation and Measurements. NMR analyses were performed on a Bruker AMX-R 300 spectrometer equipped with a broad-band probe operating at 300.13 and 121.49 MHz for ^{1}H and ^{31}P nuclei, respectively. ^{1}H chemical shifts are reported in ppm (δ) units with respect to Me_4Si and referenced to the residual protiated impurities of the deuterated solvent. Coupling constants are given in hertz. ^{31}P chemical shifts, in parts per million, are given relative to external phosphoric acid. The temperature within the probe was checked using the methanol method.[36] Slow reactions were carried out in a silica cell in the thermostated cell compartment of a rapid-scanning Hewlett-Packard Model 8452A spectrophotometer or a JASCO V-560 UV/vis spectrophotometer, with a temperature accuracy of 0.02 °C. Fast reactions required the use of an Applied Photophysics Bio Sequential SX-17 MX stopped-flow spectrophotometer.

Preparation of Complexes. *cis*-$[PtMe_2(Me_2SO)_2]$,[37] *trans*-$[PtMeCl(Me_2SO)_2]$,[37] $[PtMe_2(cod)]$,[38] $[PtMeCl(cod)]$,[38] and $[Pt_2Me_4(\mu\text{-}SMe_2)_2]$,[39] used as precursors for the synthesis of the alkylphosphane complexes, were prepared by literature methods and characterized by elemental analysis and ^{1}H and ^{31}P{^{1}H} NMR spectra. All dialkyl and monoalkyl compounds in the text were synthesized using a number of variations to the literature methods in order to improve the yield and purity of old and new compounds.

Dialkyl Substrates. The complexes *cis*-$[PtMe_2L_2]$ and $[PtMe_2(L\text{-}L)]$ (L = PEt_3,[40] $P(4\text{-}MeC_6H_4)_3$;[38] L-L = dppm,[22,41] dppe,[22,41] dppp,[22,41] dppb[22,41]) were synthesized by following a well-established general procedure: a weighed amount of *cis*-$[PtMe_2(Me_2SO)_2]$ was reacted in degassed dichloromethane with a stoichiometric amount of the phosphane, and the reaction mixture was set aside for a few hours. After evaporation of most of the solvent, the complex separated out as an oil or a solid on adding light petroleum (bp 60−80 °C) and cooling. The residue was crystallized from a suitable solvent. The identity and purity of the compounds were established by elemental analysis and by their NMR spectra. In the case of the most sterically demanding phosphanes $P(Pr^i)_3$ and $P(Cy)_3$ the solvent used was toluene and, for L = $P(Pr^i)_3$, the starting material was the dimeric complex $[Pt_2Me_4(\mu\text{-}SMe_2)_2]$.

Monoalkyl Substrates. (a) *cis*-[PtMeClL$_2$] and [PtMeCl(L-L)] Complexes. Compounds with L = PEt_3,[40] $P(4\text{-}MeC_6H_4)_3$[42] were prepared using the general procedure described by Chatt and Shaw.[40] A weighed amount of the corresponding dialkyl complex in dry ether was treated with a stoichiometric quantity of dry HCl in diethyl ether. After evaporation of the solvent the residues were crystallized as white compounds from a petroleum ether mixture. Complications arose with the bulky phosphanes L = $P(Pr^i)_3$, $P(Cy)_3$ because of the easy geometrical conversion of the *cis*-monoalkyl chloride species to their trans isomers. Therefore, a solution of a weighed amount of *cis*-$[PtMe_2L_2]$ in a 8/1 CD_3OD/CD_2Cl_2 mixture was frozen in the NMR tube and then added with a solution of DCF_3SO_3 and LiCl in CD_3OD (in a 1/10 ratio with respect to the complex). The temperature was slowly increased to 225 K, and the ^{1}H and ^{31}P NMR spectra of the ensuing *cis*-monoalkyl chloride species were recorded.

***cis*-[PtMe(Cl)(P(Pr^i)$_3$)$_2$] (2b).** ^{1}H NMR (CD_3OD/CD_2Cl_2 (8/1 v/v, T = 225 K): δ 2.52 (m, 6H, P*CH*Me$_2$), 1.29 (m, 36H, PCHMe$_2$), 0.58 (m, $^2J_{PtH}$ = 53.2 Hz, $^3J_{PH}$ = 7.0 Hz, 3H, Pt−*CH*$_3$). ^{31}P{^{1}H} NMR (CD_3OD/CD_2Cl_2, T = 225 K): δ 32.8 (d, $^1J_{PtP_A}$ = 1741 Hz, P_A trans to CH_3), 27.6 (d, $^1J_{PtP_A}$ = 4250 Hz, P_B trans to Cl).

***cis*-[PtMe(Cl)(PCy$_3$)$_2$] (3b).** ^{1}H NMR (CD_3OD/CD_2Cl_2 (8/1 v/v, T = 225 K): δ 2.72−1.54 (m, 66H, Cy), 0.67 (m, $^3J_{PH}$ = 7.6 Hz, $^2J_{PtH}$ = 56.2 Hz, 3H, Pt−*CH*$_3$). ^{31}P{^{1}H} NMR (CD_3OD/CD_2Cl_2, T = 225 K): δ 23.2 (d, $^1J_{PtP_A}$ = 1753 Hz, P_A trans to CH_3), 18.7 (d, $^1J_{PtP_A}$ = 4328 Hz, P_B trans to Cl).

Compounds with L-L = dppe, dppp, dppb were obtained by reacting a weighed amount of *trans*-$[PtMeCl(Me_2SO)_2]$ with a stoichiometric amount of the chelating phosphane in distilled and degassed CH_2Cl_2. After evaporation of most of the solvent, the complexes separated out as solids on adding light petroleum and cooling.

[PtMe(Cl)(dppb)] (8b). ^{1}H NMR ($CDCl_3$, T = 298 K): δ 7.6−7.5 (m, 8H, $H_{o,o'}$), 7.4−7.3 (m, 12H, $H_{m,m'} + H_p$), 2.5 (m, 2H, PH_β), 2.3 (m, 2H, PH_α), 1.7 (m, 2H, P$H_{\alpha'}$), 0.39 (m, $^2J_{PtH}$ = 54.3 Hz, $^3J_{PH}$ = 6.8 Hz, 3H, Pt−*CH*$_3$). ^{31}P{^{1}H} NMR ($CDCl_3$, T = 298 K): δ 19.5 (d, $^1J_{PtP_A}$ = 1711 Hz, P_A trans to CH_3), 18.7 (d, $^1J_{PtP_A}$ = 4385 Hz, P_B trans to Cl). Anal. Calcd for $PtC_{29}H_{31}ClP_2$: C, 51.83; H, 4.65. Found: C, 50.61; H, 4.69.

The reaction of *trans*-$[PtMeCl(Me_2SO)_2]$ with dppm gives quantitatively the dimer $[PtMeCl(\mu\text{-dppm})]_2$. Preparation of the pure monomer was achieved by applying the Puddephatt method to **5a**.[23]

(b) *trans*-[PtMeClL$_2$] Complexes. The compounds with L = PEt_3, $P(4\text{-}MeC_6H_4)_3$ were obtained easily by spontaneous isomerization of the corresponding cis isomers in methanol, following a well-established synthetic procedure.[43]

***trans*-[PtMe(Cl)(P(4-MeC$_6$H$_4$)$_3$)$_2$] (4c).** ^{1}H NMR ($CDCl_3$, T = 298 K): δ 7.60−7.13 (m, 24H, $PC_6H_4CH_3$), 2.33 (s, 18H, $PC_6H_4CH_3$), −0.14 (m, $^2J_{PtH}$ = 79.6 Hz, $^3J_{PH}$ = 6.5 Hz, 3H, Pt−*CH*$_3$). ^{31}P{^{1}H} NMR ($CDCl_3$, T = 298 K): δ 27.7 ($^1J_{PtP}$ = 3122 Hz). Anal. Calcd for $PtC_{43}H_{45}ClP_2$: C, 60.45; H, 5.31. Found: C, 59.66; H, 5.26.

The complexes *trans*-$[PtMeCl(PCy_3)_2]$[44] and *trans*-$[PtMeCl(PPr^i_3)_2]$,[45] were obtained as follows: a Schlenk tube equipped with a magnetic bar was charged with *trans*-$[PtMeCl(Me_2SO)_2]$ (60 mg, 0.15 mmol), phosphane (0.40 mmol), and distilled CH_2Cl_2 (10 mL). The vessel was connected to a Schlenk line, where the mixture was stirred for 4 h. The solvent was removed in vacuo, and the residue was then taken up in a minimum amount of CH_2Cl_2. Addition of diethyl ether and cooling afforded colorless crystals of **2c** and **3c**.

Kinetics. The rates of protonolysis of the dialkyl complexes **1a**−**8a** were followed by stopped-flow spectrophotometry under pseudo-first-order conditions. Since some of these complexes appear to decompose slowly in methanol at room temperature, even in the absence of acid, fresh solutions of the complexes were used for all kinetic runs. Initial concentrations of starting complex were

(35) Riddick, J. A.; Bunger, W. B.; Sakano, T. K. In *Organic Solvents*, 4th ed.; Weissberger, A., Ed.; Wiley: New York, 1986.
(36) (a) Van Geet, A. L. *Anal. Chem.* **1968**, *40*, 2227. (b) Van Geet, A. L. *Anal. Chem.* **1970**, *42*, 679.
(37) Eaborn, C.; Kundu, K.; Pidcock, A. *J. Chem. Soc., Dalton Trans.* **1981**, 933.
(38) (a) Clark, H. C.; Manzer L. E. *J. Organomet. Chem.* **1973**, *59*, 411−428. (b) Scott, J. D.; Puddephatt, R. J. *Organometallics* **1983**, *2*, 1643. (c) Puddephatt, R. J.; Rashidi, M.; Fakhroeian, Z. *J. Organomet. Chem.* **1990**, *406*, 261. (d) Yang, D. S.; Bancroft, G. M.; Dignard-Bailey, L.; Puddephatt, R. J.; Tse, J. S. *Inorg. Chem.* **1990**, *29*, 2487.
(39) Hill, G. S.; Irwin, M. J.; Levy, C. J.; Rendina, L. M.; Puddephatt, R. J. *Inorg. Synth.* **1998**, *32*, 149.
(40) Chatt, J.; Shaw, B. L. *J. Chem. Soc.* **1959**, 705.
(41) Hietkamp, S.; Stufkens, D. J.; Vrieze, K. *J. Org. Chem.* **1979**, *44*, 107−113.
(42) Cobley, C. J.; Pringle, P. G. *Inorg. Chim. Acta* **1997**, *265*, 107.
(43) Romeo, R.; Minniti, D.; Trozzi, M. *Inorg. Chem.* **1976**, *15*, 1134.
(44) Strukul, G.; Michelin, R. A. *J. Am. Chem. Soc.* **1985**, *107*, 7563.
(45) Arnold, D. P.; Bennett, M. A. *J. Organomet. Chem.* **1980**, *199*, 119−135.

in the range 0.05−0.1 mM, and pseudo-first-order conditions were achieved by having the proton concentration in at least 10-fold excess. Rate constants were evaluated using the Applied Photophysics software package[46] and are reported as average values from five to seven independent runs. Second-order rate constants for the protonolysis (k_H) at 298.2 K were obtained by least-squares regression analysis of the linear plots of the pseudo-first-order rate constants vs the concentration of acid. At other temperatures, the values of k_H were obtained from the ratio of the measured pseudo-first-order rate constants k_{obs} to $[H^+]$. Enthalpies and entropies of activation for protonolysis were derived from a linear least-squares analysis of $\ln(k_H/T)$ vs T^{-1} data.

The slowest protonolysis reactions of the complexes *cis*-$[PtMeClL_2]$ (**1b**−**4b**), $[PtMeCl(L\text{-}L)]$ (**5b**−**8b**), and *trans*-$[PtMeClL_2]$ (**1c**−**4c**) were followed by conventional spectrophotometry by repetitive scanning of the spectrum at suitable times in the range 320−220 nm or at a fixed wavelength, where the absorbance change was largest. The reaction was started by mixing known volumes of the complex and of HCF_3SO_3, in the presence of known amounts of lithium chloride, in a 1 cm quartz cell placed in the thermostated cell compartment of the spectrophotometer. The ionic strength was adjusted using lithium perchlorate to $I(LiClO_4) = 0.2$ M. Alternatively, the monoalkyl chloride complexes **1b**−**8b** were generated in situ in a silica cell by adding with a syringe a prethermostated solution of $[PtMe_2L_2]$ to a methanolic thermostated solution of HA and LiCl, taking advantage of the very fast cleavage of the first Pt−Me bond. Likewise, the trans complexes **1c**−**4c** were generated in situ from protonolysis of **1a**−**4a** with HA and addition of lithium chloride only when the ensuing cis−trans isomerization of the cationic solvento complex *cis*-$[PtMeL_2(MeOH)]^+$ was complete.[6k,13] Rate constants were evaluated with the SCIENTIST[47] software package by fitting the absorbance/time data to the exponential function $A_t = A_{00} + (A_0 - A_{00}) \exp(-k_{obs}t)$. Rate constants are reported as average values from five to seven kinetic runs.

Kinetic Isotope Effect. The kinetic isotope effect was determined systematically by comparing the rates of reactions carried out in CH_3OH and in CH_3OD. Thus, kinetic runs were carried out with DOTf and LiCl in CH_3OD by following exactly the same procedure described above for stopped-flow and conventional spectrophotometric measurements.

Detection of Platinum(IV) Alkyl Hydrido Species. An appropriate amount of the complex (5−6 mg, 0.01 mmol) was combined with Ph_4AsCl (42 mg, 0.1 mmol). The reagents were dissolved in CD_2Cl_2 (0.5 mL) and then cooled to −78 °C before adding via syringe HOTf (0.1 mmol) in CD_2Cl_2. After the contents were mixed while the tube was kept as cool as possible, the tube was placed in the precooled NMR probe. Relevant ^1H and ^{31}P NMR data for some identified $[PtMeCl_2(H)L_2]$ species are given in Table 2.

H/D Exchange. A similar procedure was applied to reveal H/D exchange in methanol. Thus, the complex was dissolved in a CD_3OD/CD_2Cl_2 mixture (8/1) and cooled to −48 °C. After addition of a solution of DOTf the mixture was placed in the NMR probe. Deuterium incorporation into the methyl positions was checked at this temperature for all compounds studied. The phenomenon was monitored only for compounds **1c**−**3c,** after addition of a small excess of LiCl and warming to −20 °C, by the loss in the integration intensity of the Pt−Me resonance and, at higher temperatures, by the observation of the release of the full range of methane isotopomers.

Acknowledgment. We are grateful to the Ministero dell'Università e della Ricerca Scientifica e Tecnologica (MIUR), PRIN 2004, and to the University of Messina, PRA 2003, for funding this work.

Supporting Information Available: A figure showing typical ^1H and ^{31}P NMR features useful in distinguishing between compounds of classes **a**−**c**, text giving a full listing and assignment of ^1H and ^{31}P NMR data for compounds of classes **a**−**c**, and tables giving the concentration and temperature dependence of primary kinetic data. This material is available free of charge via the Internet at http://pubs.acs.org.

OM060217N

(46) Applied Photophysics Bio Sequential SX-17 MV, sequential stopped-flow ASVD spectrofluorimeter. Software manual: Applied Photophysics, Kingstone Road, Leatherhead KT22, U.K.

(47) SCIENTIST; Micro Math Scientific Software, Salt Lake City, UT.